ASERS

Journal of Environmental Management and Tourism

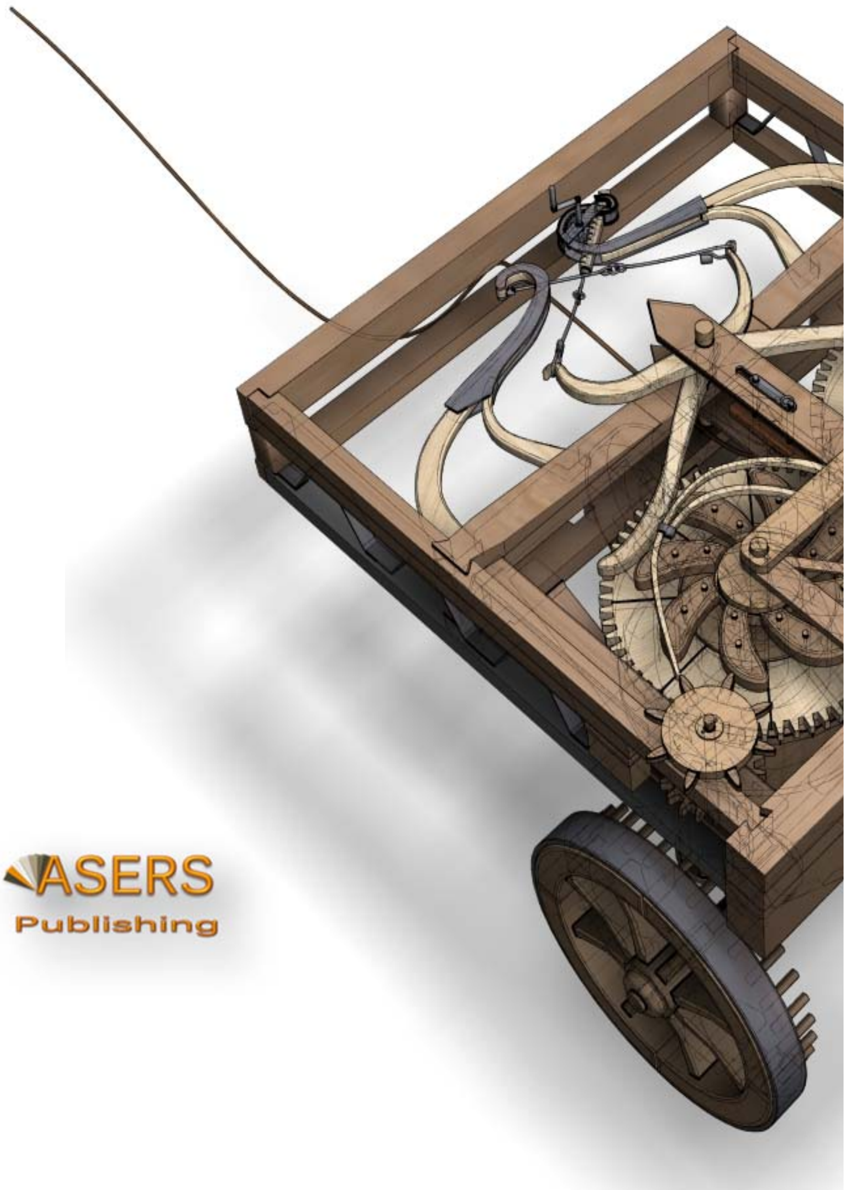

Quarterly
Volume X
Issue 1(33)
Spring 2019
ISSN 2068 – 7729
Journal DOI
https://doi.org/10.14505/jemt

ASERS Publishing

Spring 2019
Volume X
Issue 1(33)

ASERS Publishing
http://www.asers.eu/asers-publishing
ISSN 2068 – 7729
Journal DOI: https://doi.org/10.14505/jemt

Table of Contents:

Spring 2019
Volume X
Issue 1(33)

ASERS Publishing
http://www.asers.eu/asers-publishing
ISSN 2068 – 7729
Journal DOI: https://doi.org/10.14505/jemt

Call for Papers
Summer Issues 2019
Journal of Environmental Management and Tourism

Journal of Environmental Management and Tourism is an interdisciplinary research journal, aimed to publish articles and original research papers that should contribute to the development of both experimental and theoretical nature in the field of Environmental Management and Tourism Sciences.

Journal will publish original research and seeks to cover a wide range of topics regarding environmental management and engineering, environmental management and health, environmental chemistry, environmental protection technologies (water, air, soil), pollution reduction at source and waste minimization, energy and environment, modeling, simulation and optimization for environmental protection; environmental biotechnology, environmental education and sustainable development, environmental strategies and policies, etc. This topic may include the fields indicated above, but are not limited to these.

Authors are encouraged to submit high quality, original works that discuss the latest developments in environmental management research and application with the certain scope to share experiences and research findings and to stimulate more ideas and useful insights regarding current best-practices and future directions in environmental management.

Journal of Environmental Management and Tourism is indexed in SCOPUS, RePEC, CEEOL, ProQuest, EBSCO and Cabell Directory databases.

All the papers will be first considered by the Editors for general relevance, originality and significance. If accepted for review, papers will then be subject to double blind peer review.

Deadline for submission:	26th May 2019
Expected publication date:	June 2019
Website:	https://journals.aserspublishing.eu/jemt
E-mail:	jemt@aserspublishing.eu

To prepare your paper for submission, please see full author guidelines in the following file: JEMT_Full_Paper_Template.docx, then send it via email at jemt@aserspublishing.eu.

Volume X, Issue 1(33) Spring 2019

ASERS Publishing

DOI: https://doi.org/10.14505/jemt.10.1(33).14

Implications for Provenance since the Last Glaciations in Southeastern Andaman Sea Sediments by Clay Mineralogy

Suratta BUNSOMBOONSAKUL
Department of Marine Science, Faculty of Science, Chulalongkorn University, Thailand
State Key Laboratory of Marine Geology, Tongji University, China
suratta.b@gmail.com

Penjai SOMPONGCHAIYAKUL[3]
Department of Marine Science, Faculty of Science, Chulalongkorn University, Thailand
penjai.s@chula.ac.th

Zhifei LIU
State Key Laboratory of Marine Geology, Tongji University, China
lzhifei@tongji.edu.cn

Akkaneewut CHABANGBORN
Department of Geology, Faculty of Science, Chulalongkorn University, Thailand
akkaneewut@gmail.com

Anond SNIDVONGS
Geoinformatics and Space Technology Development Agency, Thailand
Anond@gistda.or.th

Suggested Citation:
Bunsomboonsakul, S. *et al.* (2019). Implications for Provenance since the Last Glaciations in Southeastern Andaman Sea Sediments by Clay Mineralogy. *Journal of Environmental Management and Tourism*, (Volume X, Spring), 1(33): 140-148. DOI:10.14505/jemt.v10.1(33).14

Article's History:
Received January 2019; *Revised* February 2019; *Accepted* March 2019.

Abstract

This study presents high-resolution clay mineralogy of Core MASS-III-10, located in the southeastern Andaman Sea. The study aimed to investigate terrigenous sedimentary input from various potential provenances throughout different periods of geological time. The clay mineral assemblages of MASS-III-10 reveal a high amount of smectite at 73% (65-79%), a moderate kaolinite at 12% (10-17%), and a low illite and chlorite content(<15%) over the last 45 ka. Provenance analysis suggests the most fine-grained terrigenous sediments originated from the Irrawaddy Delta Shelf (IDS), with minor sediments deriving from the Andaman Islands, the East Continental Shelf (ECS), and Sumatra provenance. The results show that IDS were predominantly smectite (~44%) while the ECS largely produced kaolinite (47%). The provenance interpretation based on the smectite content revealed that over time there has been no change in the main source of sediment in the Andaman Sea, despite changes in the volume of sedimentary input. Since the last glaciation, the Myanmar provenance (including IDS) has always contributed clay minerals, while other sources made up only minor contributions to the Andaman Sea. The clay minerals from the Myanmar provenance increased when the sea level was at a low stand (MIS 2), potentially due to shoreline retreat which enabled easier transportation of sediment from other sources. During the interglacial period (MIS 1 and 3), the study found a decrease in Myanmar-sourced clay minerals, which may be because the higher sea level made clay mineral deposition more difficult.

Keywords: The Andaman Sea; clay mineral; provenance; last glaciations; terrigenous sediment.

JEL Classification: Q24; Q25; Q39.

[3] Corresponding author

Introduction

The Andaman Sea occupies a unique position as a marginal basin in Southeast Asia geography (Khan and Chakraborty 2005, 259-71). The Andaman Sea basin and the studied area in particular, are considered to be a semi-enclosed sea which extends to the Mergui Basin in the southeastern Andaman Sea (Curray *et al.* 2005, 187-232). The continental shelf extends from the northern section of the Irrawaddy delta and along the eastern section towards the south which is connected to the Strait of Malacca, and is mostly underlined by sedimentary input. The stability of the morphological equilibrium in the Andaman Sea basin is based on a balance of hydrodynamic sedimentation processes of erosion and deposition in the different geological settings.

Since the southeastern Andaman Sea is defined by stable sedimentation underlying the supplied sediment, sediment deposition can be investigated to understand the terrigenous sedimentary inputs from the sediment sources surrounding the Andaman Sea. In the past, provenance analysis was focused on the general mineralogical properties of sand and sandstone samples, as well as on the specific content of distinctive heavy minerals. In particular, heavy minerals were used as fingerprints for sediment source areas, and so were useful when attempting to reconstruct the parent rocks in the source erosion regions (Allen 2008, 274-6). Current geochemical methods are comparatively better suited for provenance study, with clay mineralogy regularly being studied to reconstruct paleo-environmental evolution at different timescales. Clay mineral assemblages also provide information about the weathering environment since the relative formation of particular clay minerals depends on the balance between physical erosion and chemical weathering in the source regions, prior to the erosion and transportation of the material to the ocean (Thiry 2000; Chamley 1989). Paleo-climatology is the study of past climates, which relies on the use of imprints created during previous climates, known as proxies, to interpret paleo-climate since it is not possible to go back in time and see what the climate were like. Different timescales can be used to investigate specific features, for example weathering history can be indicated by long-term variations, while shorter timescales allow the study of variations in erosion products which are directly related to changes to the variation of precipitation (*e.g.* Jiwarungrueangkul *et al.* 2019, 127-37; Sang *et al.* 2018, 1-24)

Nonetheless, there is relatively poor documentation of multi-proxy studies of sediment cores in the Andaman Sea (*e.g.* Ali *et al.* 2015, 505-21; Cao *et al.* 2015, 512-25; Awasthi *et al.* 2014, 3890-906; Sijinkumar *et al.* 2010, 221-9; Rashid *et al.* 2007, 2586-97; Colin *et al.* 2006, 1999, 1998). Only one study provide a long-term record for the last 280 ka (Colin *et al.* 1999, 647-60).The Andaman Sea is therefore a particularly interesting area for paleo-environmental and sedimentological study. A study on the high-resolution terrigenous sediments such as clay minerals has therefore been suggested in this area. The main research objectives of the present study are to reveal the clay mineralogy of the surface sediments of the Andaman Sea to understand the possible transportation processes, to explore the clay mineral variation since the last glaciation, and to reconstruct the paleo-environmental climate evolution that has been driven by climate change since the last glaciation.

1. Materials and Methods

The core MASS-III-10 was taken during the MASS-III cruise in January 2011 by the R/V Charkratong Tongyai. This core was taken from the Andaman Sea outer shelf (located at 8° 06.92' N, 95° 51.74' E) using gravity coring using a 1.5 m long core at a water depth of 630 m. (Figure 1). The sediment lithology of MASS-III-10 consisted of a silt layer at the top, and clay layers with several intervals rich in foraminifera, and shell fragment layers. No turbidity layer in the sediment sequence was found in MASS-III-10.

Of the surface sediments retrieved by grab samplers, there were 39 samples taken from the Irrawaddy Delta Shelf (IDS) in Myanmar in December 2009, while 22 samples were collected from the Eastern Continental Shelf (ECS) of the Andaman Sea in Thailand (Figure 1). The IDS location is at the confluence of two major river systems which have actively supplied sediment into the Andaman basin, with the Salween River in the east and the Irrawaddy River to the west. The 22 ECS samples were collected nearshore of Phang-Nga province in December 2008. The sample sites were assumed to be well-preserved areas of undisturbed-sediment since the collection locations are far from human activities.

Clay mineralogy was analyzed by X-ray diffraction (XRD) using a PANalytical diffractometer. The core sediment and surface sediment samples were prepared first by sieving the sediment at 63 um to sort the shell fragments, and then by extracting the carbonate ion by acid treatment to produce carbonate-free sediment (Liu *et al.* 2009). Non-calcareous clay-sized samples(<2 μm) were individually measured under three conditions; (i) air-drying, (ii) ethylene-glycol solvation for 24 hours, and (iii) heating at 490°C for 2 hours (Holtzapffel 1985). Clay mineral identification and calculation were on the basis of an XRD overlay under three test conditions (Liu *et al.*

2004). The semi-quantitative parameters of each peak diagram were calculated using the MacDiff software (Petschick 2000) on the ethylene glycol curve. The relative error was approximately ±5% (Holtzapffel 1985), while the precision of the replicate samples was analyzed for ±2% (2σ) (Liu *et al.* 2010). This study utilized high-resolution clay mineral analysis at a 2 cm resolution, which was performed at the State Key Laboratory of Marine Geology, Tongji University, Shanghai, China.

Figure 1. The Andaman Sea location combined with a contour map by ETOPO1 Bedrock: a) sitemap of sediment sample locations in the Andaman Sea, b) the star symbols are sediment cores, while the triangle symbols represent the surface sediments used in this study.

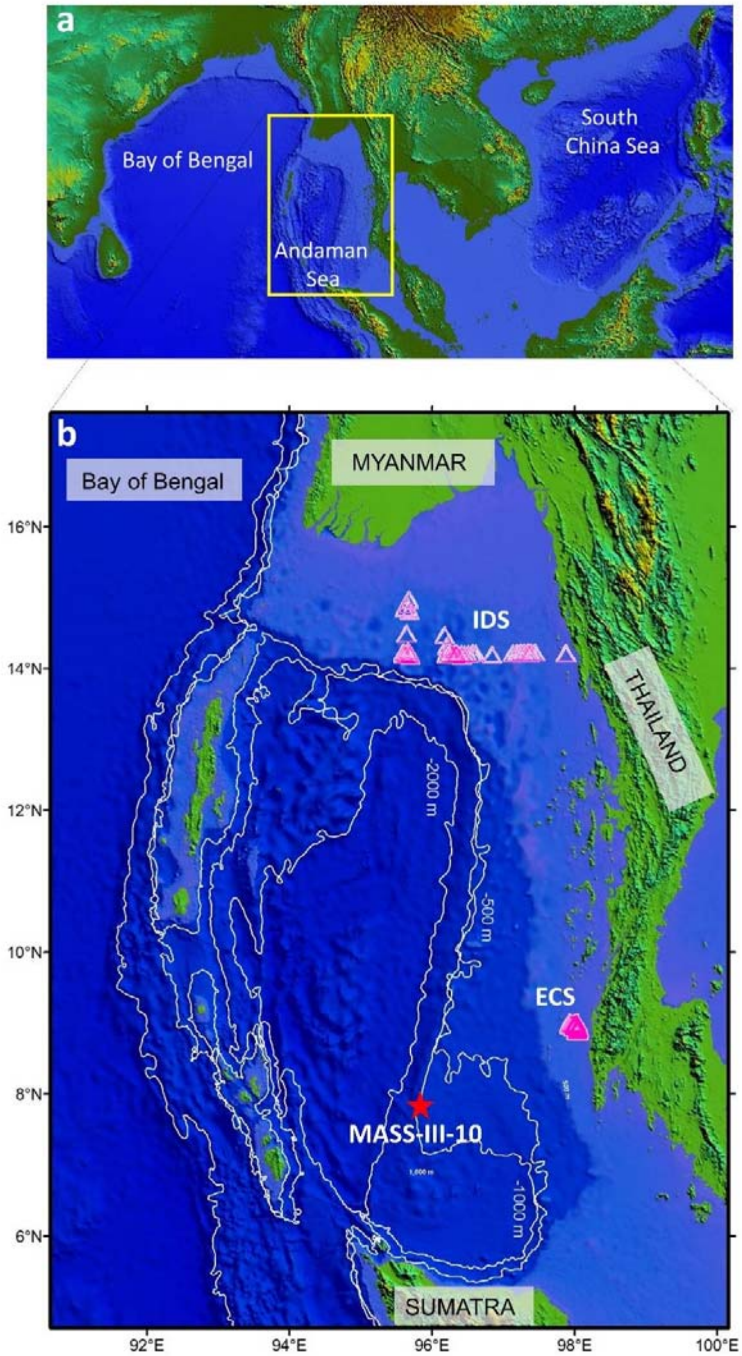

2. Results and Discussion

2.1 Age-Depth Model of Core MASS-III-10

The ^{14}C-AMS dating and oxygen isotope ($\delta^{18}O$) stratigraphy were obtained by *Globigerinoides ruber* (*G. Ruber*), while bulk carbonate content was employed to establish the age models of core MASS-III-10. The obtained ^{14}C dates were converted into geological calendar ages using the Marine 09 calibration curve (Reimer *et al.* 2009) and then calibrated using Calib 7.0.2 (Stuiver *et al.* 1998) within 1σ level of error. The analysis linked together the reference curve, core MD77-169 (the only core in the Andaman Sea which provides a semi-continuous record for the last 280 ka), and the $\delta^{18}O$ curves of the core used in this study, as shown in Figure 2. Five ^{14}C-AMS samples were obtained (Table 1). MASS-III-10 revealed that the ages cover the late glaciation period (~45 ka) and the Holocene. The resultant ^{14}C calibrated ages cover the MIS 3 and MIS 2 for glacial variations, and the MIS 1 for interglacial variations (Figure 2).

Table 1. Five ^{14}C-AMS ages of MASS-III-10, calibrating by Marine09 calibration curve (Reimer *et al.* 2009) with 1σ level of errors. MASS-III-10 was revealed age covers since late glaciation (~45 ka) and Holocene.

Depth (cm)	Foraminifera species	^{14}C-AMS age BP	Average Calibrated age (1σ, yrs BP)	Error 1 σ
MASS-III-10				
12	G. ruber	6,410 ± 40	4,940	118
24	G. ruber	15,110 ± 60	15,953	189
60	G. ruber	27,640 ± 130	29,217	195
88	G. ruber	30,480 ± 180	32,162	354
142	G. ruber	41,950 ± 690	43,019	1,201

Figure 2. Lithographic descriptions of the core MASS-III-10 with the XRF core scanner image (left). The age model of the core MASS-III-10 (right) is based on ^{14}C-AMS dating, total carbon content, and the oxygen isotopic ratios ($\delta^{18}O$) displayed according to depth (cm) vs age (ka). The triangle symbols represent controlling points of the ^{14}C calibrated age. The bulk of the carbonate content and the $\delta^{18}O$ stratigraphy record of *G. ruber* are represented against depth.

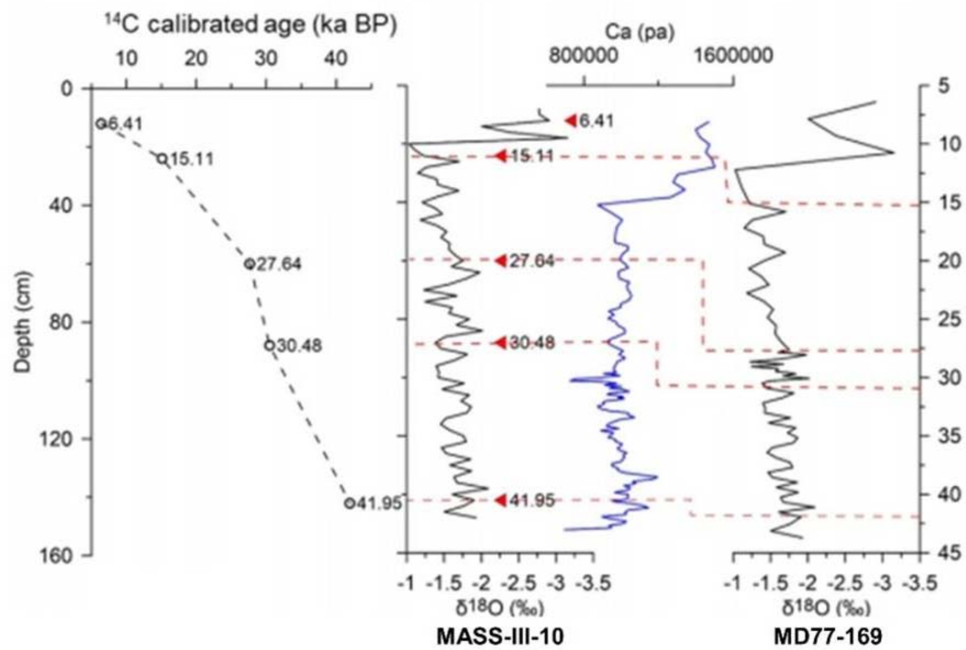

2.2 Clay Minerals of Core MASS-III-10

The relative clay mineral proportions of the core and surface sediments were calculated according to the percentage of the total clay assemblage, including the amount of smectite, kaolinite, illite and chlorite, and also based on the illite crystallinity and the illite chemical index. The clay mineral assemblage of MASS-III-10 over the last 45 ka is plotted in Figure 3. The sediments of core MASS-III-10 contain a high amount of smectite at 73% (65-79%), a moderate amount of kaolinite at 12% (10-17%), and a low amount of illite and chlorite content

(<15%). In general, the smectite distribution was inversely correlated to illite. The sediments from MIS 3 and MIS 2 were characterized by higher smectite than MIS 1, whereas illite was lower during MIS1 compared to MIS 3 and MIS 2. Meanwhile, kaolinite and chlorite displayed little change since 45 ka.

For the downcore variation between ~40 to 34 ka, smectite was dominant in the clay content at 73%, which followed a decreasing trend after 39 ka. The smectite variation during this period decreased from 76% to 73% and presented a gradual decrease. Meanwhile, the variation of the illite content decreased from the previous period (45 ka to 39 ka) before fluctuating. Illite reached a high peak after 35 ka and a further small peak around 32 ka, which corresponds well with the kaolinite variation. Similarly, the lowest peak of chlorite variation was reached at ~37 ka before increasing again at 35 ka. In addition, the smectite/(illite+chlorite) ratio which was reported to represent the changing minerals within the clay fraction, reached its highest peak at 37 ka due to the low illite and chlorite content. In contrast, the kaolinite variation clearly fluctuated. The mean kaolinite content reached a peak of 13% at 37 ka, before dropping to 1% at 35 ka, and then returning to 13% at 34 ka.

Smectite was also the dominant clay content during the Last Glacial Maximum (LGM) (23 to 19 ka), and followed a decreasing trend after 23 ka before increasing its content proportion in the Holocene. The illite and chlorite content showed an inverse trend to the smectite content. By contrast with smectite, the illite content presented an increasing amount of variation, and its content was lower during the LGM compared to the Holocene. The chlorite variation presented a slow rate of variation and a low content ~22 ka. Accordingly, the smectite/(illite+chlorite) ratio decreased. During the same stage, the variation of kaolinite revealed the highest content percentage of 15% at 20 ka. With the exception of smectite, the average mineral content of illite, chlorite, and kaolinite was higher during MIS 3 than the LGM.

Figure 3. Summary results of the MASS-III-10. Clay mineral assemblages (%) for <2 μm particles non-calcareous clay; kaolinite, chlorite, illite, smectite, ratio of smectite/(illite+chlorite) (blue), illite chemical index, and illite crystallinity versus age (ka).The grey bar represents the MIS 2 stage and LGM period was presented by the red line. ^{14}C-AMS dating point were displayed by the green arrows.

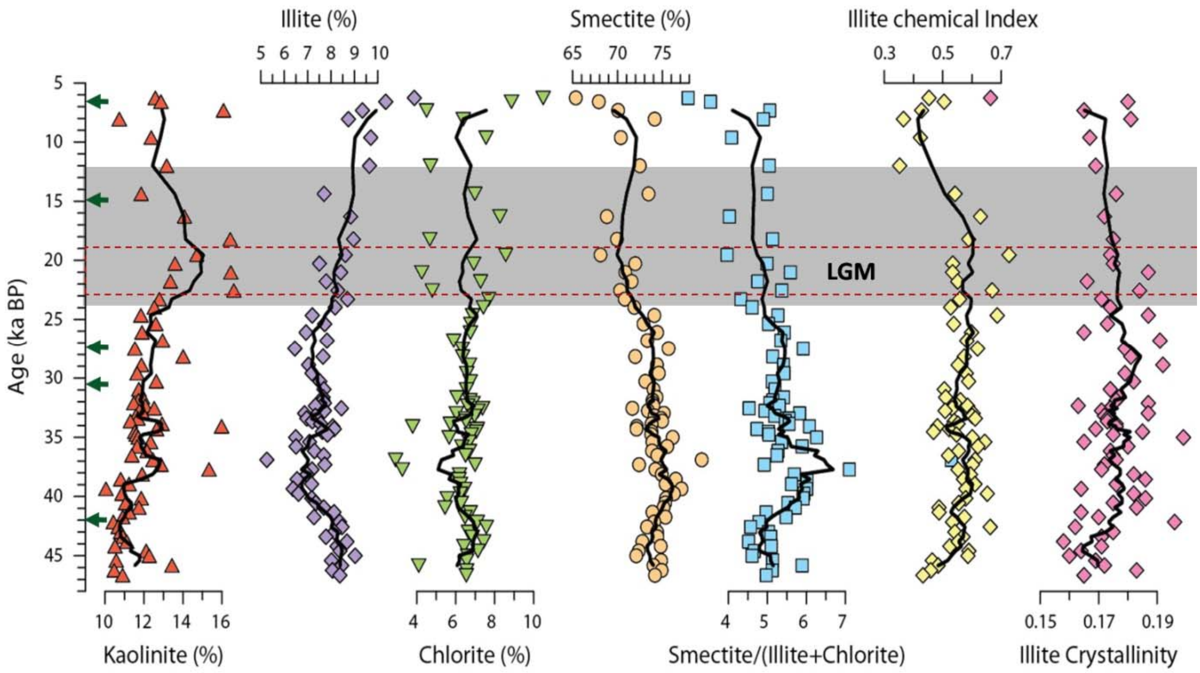

2.3 Clay Minerals in the Surface Sediments

The clay mineral determination of the IDS sample suggests a dominance of the smectite fraction of about 40-55% (Figure 4). Meanwhile, the concentrations of illite, chlorite, and kaolinite varied between 30-15%, 22-10%, and 20-14%, respectively (Figure 4). The concentration of smectite gradually increased between 42% and 54% along a transect running from the west to the east of the IDS (Figure 4b). By contrast, the illite and chloride components declined from 25% to 18% and from 18% to 12%, respectively. Figure 3 showed that the kaolinite fractions changed only slightly by about 14%. The illite chemistry index increased from 0.4 in the west to 0.5 in the east of the IDS (Figure 4).

The most abundant clay mineral in the surface sample obtained from the ECS was kaolinite, which varied from 30% to 60% (Figure 4). The smectite fraction, the dominant clay mineral assemblage in the IDS, was about 22% and there was clear variation between <5 to >50%. Illite and chlorite concentrations ranged from 22% to 12%, and 7% to 15%, respectively. Finally, the illite chemistry ratio was about 0.3.

Figure 4. a) Distribution of average clay mineral assemblages (%) of the four main clay contents are indicated by different colors; smectite (blue), illite (yellow), chlorite (green), and kaolinite (red), b) the plot of the clay mineral assemblages (%), showing the percentage of the kaolinite, chlorite, illite, smectite, and illite chemistry individual indexes every 2 cm against the longitude (degrees E). The clay mineral determinations (n = 39 individual samples) were composed of longitudinal data from the west to the east of the Irrawaddy Delta Shelf (IDS) in Myanmar.

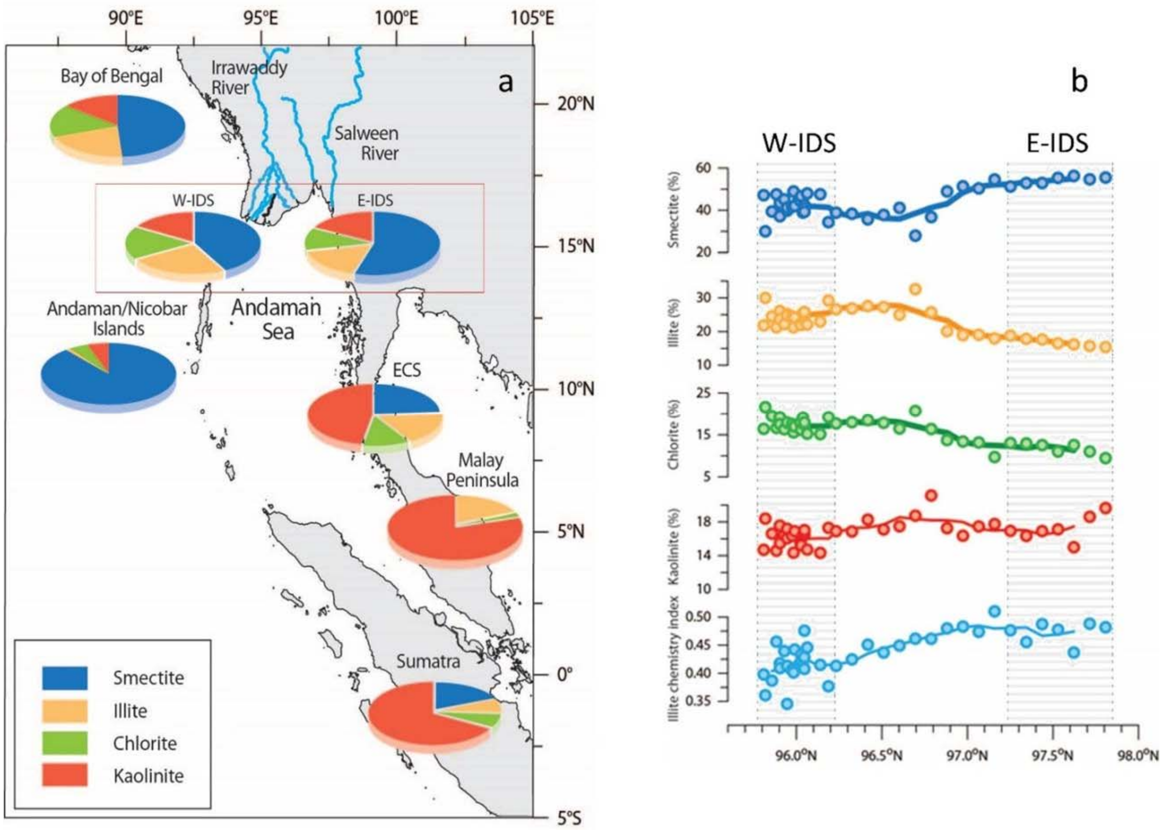

2.4 Provenance Analysis

The clay mineralogy of surface samples from the Andaman Sea and the surrounding area were investigated to reveal the source of detrital fine-grained sediments. Three characteristic end-members (smectite, kaolinite, and illite+chlorite) in the clay mineral compositions were characterized to identify the potential provenances of the fluvial input. The clay mineral assemblages in the Andaman Sea and surrounding fluvial drainage basins revealed differences between the provenances. The clay mineral compositions were therefore grouped into four different provenances according to the average clay mineral assemblages, as shown in Figure 5.

The dominance of smectite in the surface sediment was influenced by the prevailing surface circulation and the differential settling of smectite. As per Figure 5, the core sediment group in 5b corresponds with the IDS group from the Myanmar shelf, suggesting that the clay mineral in the downcore was under lithological forcing, similar to the core top sediment (Figure 5b). It could be suggested that the sediment that dispersed to the core sites came from the Myanmar shelf, the rest area of the sediment that eroded from the Irrawaddy and Salween Rivers.

Figure 5. Ternary diagram of the averaged clay mineral assemblages by three end members; illite+chlorite, kaolinite and smectite of the surface and core sediments were displayed in different shades. a) Two provenances are plotted in the diagram as IDS and ECS. The clay mineral controlling factors are displayed as blue arrows. b) The core top sediments of core MASS-III-10 and MD77-169 were included to represent modern sedimentary deposition at the core sites along with the different provenances. c) The clay mineral assemblages of MASS-III10 were presented according to the different timescales, with the purple circle representing the Holocene sediment, and the red triangle representing the glacial sediment.

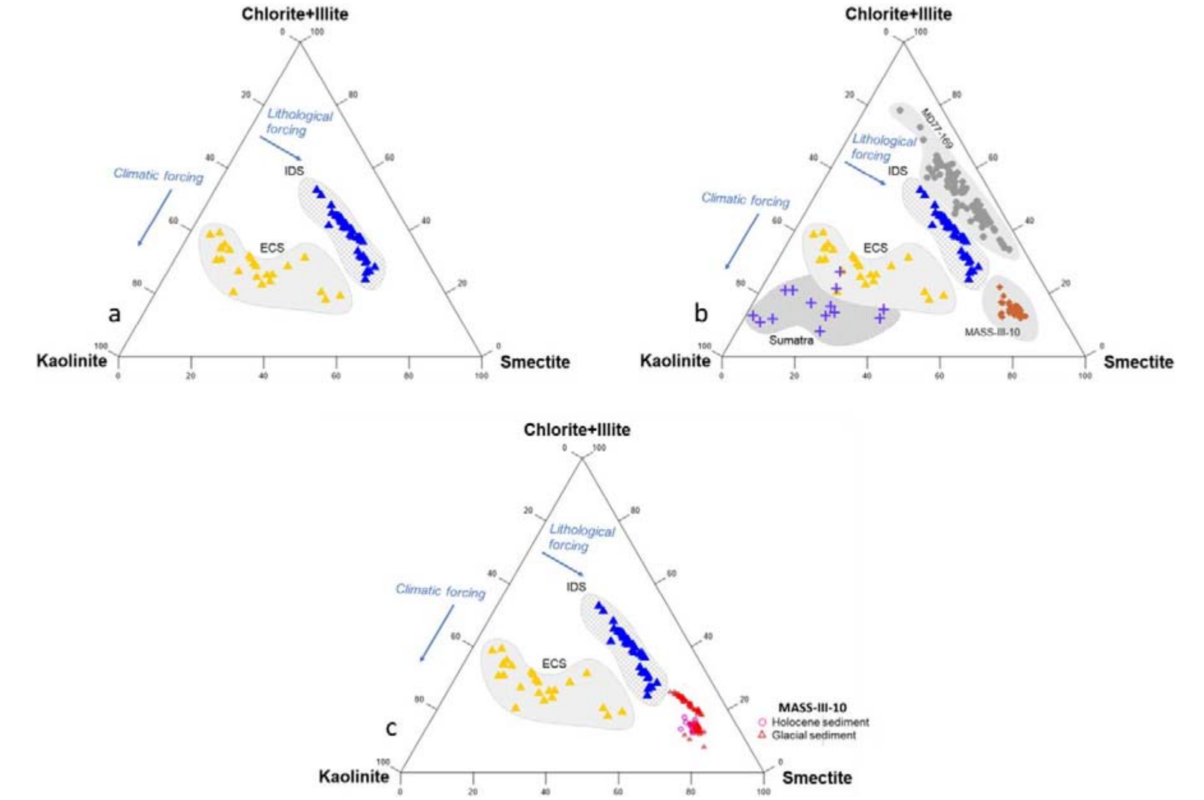

Moreover, the large downcore variations of MASS-III-10 suggest that the relative contributions from the different source areas may be related to monsoon changes throughout the glaciation period and the Holocene (Awasthi *et al.* 2014, 3890-906). The changing source contributions at the core location was most likely influenced by surface currents acting as sediment transportation, as indicated by variations in the sedimentation rate between the sediment cores. The sedimentation rate in the deep sea can be affected by various processes, such as the dynamics of transportation from land, surface circulation patterns, as well as local processes like turbidity by channel transportation and sea level changes. However, in the northern Indian Ocean in particular, the sedimentation rate was mostly affected by physical weathering, such as continental erosion linked to the intensity of summer monsoons (Joussain *et al.* 2016; Cao *et al.* 2015; Awasthi *et al.* 2014; Chauhan and Vogelsang 2006, 379-86).Consistent with previous studies, the provenance analysis suggests that the Irrawaddy and Salween Rivers have been the main sediment sources for the Andaman Sea over the last 45 ka (Ali *et al*. 2015; Cao *et al.* 2015; Awasthi *et al.* 2014; Colin 2006, 1999, 1998). Nonetheless, Colin *et al.* (2006; 1999) suggest that sedimentary inputs into the northern Andaman Sea have not varied over the past 60 ka. However, Figure 5c reveals sediment input variation during the glacial and interglacial (Holocene) periods recorded in core MASS-III-10, suggesting varying sedimentary contributions at the core site. This could be due to changes to other controlling factors, such as river discharge.

Conclusion

The clay mineral assemblage of the IDS is largely composed of smectite (44%), and moderate amounts of kaolinite (17%), chlorite (16%) and illite (13%). Meanwhile, the clay minerals of the ECS consist of mostly kaolinite (47%), and moderate amounts of smectite (23%), chlorite (18%) and illite (11%). In comparison with other potential provenance areas, the clay mineral assemblages of the surface sediments show two significant features: (1) a high smectite content (47%) in the IDS in Myanmar and extremely high values (>90%) in the

Andaman Islands; (2) high kaolinite content (generally >60%) in Sumatra, extremely high values (~80%) in the Malay Peninsula, and >40% in the ECS.

The clay mineral assemblages of MASS-III-10 consist of high smectite contents at 73%, while the kaolinite content is a minor mineral at 12%, and illite and chlorite make up ~15%. A downcore variation of clay mineral content is recorded in the core MASS-III-10 over the last 45 ka, including during the LGM and the Holocene periods. The core reveals that the amount of smectite in the Holocene (65-78%) was lower than the LGM (51-70%), while kaolinite increased since the last glaciation. The proportions of illite and chlorite show a similar trend in the downcore distribution, with their values reaching a peak during the Holocene.

Consequently, the high proportion of smectite deposition in MASS-III-10 suggests that the smectite inputs in the northern and western parts of the Andaman Sea and the Andaman Islands are potentially largely derived from the Irrawaddy and Salween River systems in Myanmar. Moreover, the smectite distribution pattern in MASS-III-10 is clearly similar to the Myanmar group. Meanwhile, the kaolinite is mostly derived from the Malay Peninsula and Sumatra, which are related to the extremely strong chemical weathering processes in these two regions. The dominance smectite in the surface sediment is influenced by the prevailing surface circulation and the differential settling of smectite. This corresponded well with the Myanmar shelf sediment, suggesting that the clay mineral in the downcore was under lithological forcing, similar to the core top sediment. This may suggest that the sediment that dispersed to the core sites originated from the Myanmar shelf, which acts as a rest area for eroded sediment from the Irrawaddy and Salween Rivers.

Acknowledgments

We would like to especially thank the research project ''Morphodynamics and Slope Stability of the Andaman Sea Shelf Break (MASS)'' for sediment material that was provided. We specially thank to State Key Laboratory of Marine Geology, Tongji University for laboratory performs. This work was supported by Professor Dr. Zhifei Liu project funding.

References

[1] Ali, S., *et al.* 2015. South Asian monsoon history over the past 60 kyr recorded by radiogenic isotopes and clay mineral assemblages in the Andaman Sea. *Geochemistry, Geophysics, Geosystems,* 16(2): 505-521.

[2] Allen, P. A. 2008. From landscapes into geological history. *Nature*, 451(7176): 274-276.

[3] Awasthi, N., *et al.* 2014. Provenance of the late quaternary sediments in the Andaman Sea: implications for monsoon variability and ocean circulation. *Geochemistry Geophyics Geosystems*, 15(10): 3890-3906.

[4] Cao, P., *et al.* 2015. Sedimentary responses to the Indian Summer Monsoon variations recorded in the southeastern Andaman Sea slope since 26 ka. *Journal of Asian Earth Sciences*, 114: 512-525.

[5] Chamley, H. 1989. *Clay Sedimentology*. Springer, Berlin: 623 pp.

[6] Chauhan, O. S., and Vogelsang, E. 2006. Climate induced changes in the circulation and dispersal patterns of the fluvial sources during late quaternary in the middle Bengal Fan. *Journal of Earth System Science*, 115(3): 379-386.

[7] Colin, C., Kissel, C., Blamart, D., and Turpin, L. 1998. Magnetic properties of sediments in the Bay of Bengal and the Andaman Sea: impact of rapid North Atlantic Ocean climatic events on the strength of the Indian monsoon. *Earth Planetary Science Letters,* 160: 623-635.

[8] Colin, C., Turpin, L., Bertaux, J., Desprairies, A., and Kissel, C. 1999. Erosional history of the Himalayan and Burman ranges during the last two glacial-interglacial cycles. *Earth and Planetary Science Letters*, 17: 647-660.

[9] Colin, C., *et al.* 2006. Evolution of weathering patterns in the Indo-Burman Ranges over the last 280 kyr: Effects of sediment provenance on 87Sr/86Sr ratios tracer. *Geochemistry, Geophysics, Geosystems*, 7.

[10] Curray, J. R. 2005. Tectonics and history of the Andaman Sea region. *Journal of Asian Earth Sciences,* 25(1): 187-232.

[11] Holtzapffel, T. 1985. Les *Minéraux Argileux: Préparation, Analyse Diffractométrique et Détermination*. Société Géologique du Nord Publications 12: 136 pp.

[12] Jiwarungrueangkul, T., Liu, Z., and Zhao, Y. 2019. Terrigenous sediment input responding to sea level change and East Asian monsoon evolution since the last deglaciation in the southern South China Sea. *Global and Planetary Change,* 174(2019): 127-137.

[13] Joussain, R., *et al.* 2016. Climatic control of sediment transport from the Himalayas to the proximal NE Bengal Fan during the last glacial-interglacial cycle. *Quaternary Science Reviews,* 148: 1-16.

[14] Khan, P. K., and Chakraborty, P. P. 2005. Two-phase opening of Andaman Sea: a new seismotectonic insight. *Earth and Planetary Science Letters*, 229(3-4): 259-271.

[15] Liu, Z., *et al.* 2010. Clay mineral distribution in surface sediments of the northeastern South China Sea and surrounding fluvial drainage basins: Source and transport. *Marine Geology*, 277: 48-60.

[16] Liu, Z., *et al.* 2004. Erosional history of the eastern Tibetan Plateau since 190 Kyr ago: clay mineralogical and geochemical investigations from the southwestern South China Sea. *Marine Geology*, 209: 1-18.

[17] Liu, Z., *et al.* 2009. Chemical weathering in Luzon, Philippines from clay mineralogy and major-element geochemistry of river sediments. *Applied Geochemistry*, 24(11): 2195-2205.

[18] Petschick, R. 2000. Unpublished computer program. Mac Diff 4.2.3., Johann-Wolfgang Goethe Universitat, Available at: http://servermac.geologie.unfrankfurt.de/Rainer.html2000

[19] Rashid, H., Flower, B.P., Poore, R.Z., and Quinn, T.M. 2007. A ~25 ka Indian Ocean monsoon variability record from the Andaman Sea. *Quaternary Science Reviews,* 26(19-21): 2586-2597.

[20] Reimer, P. J., *et al.* 2009. IntCal09 and Marine09 radiocarbon age calibration curves, 0-50,000 years CAL BP. *Radiocarbon*, 51(4): 1111-1150.

[21] Sang, P.N., *et al.* 2018. Chemical weathering in central Vietnam from clay mineralogy and major-element geochemistry of sedimentary rocks and river sediments. *Heliyon*, 4(2018) e00710: 1-24.

[22] Sijinkumar, A. V., Nath, B. N., and Guptha, M. 2010. Late Quaternary record of pteropod preservation from the Andaman Sea. *Marine Geology*, 275(1): 221-229.

[23] Stuiver, M., *et al.* 1998. INTCAL98 radiocarbon age calibration, 24,000-0 cal BP. *Radiocarbon*, 40(3): 1041-1083.

[24] Thiry, M. 2000. Palaeoclimatic interpretation of clay minerals in marine deposits: An outlook from the continental origin. *Earth Science Reviews,* 49(1-4): 201-221.

ASERS

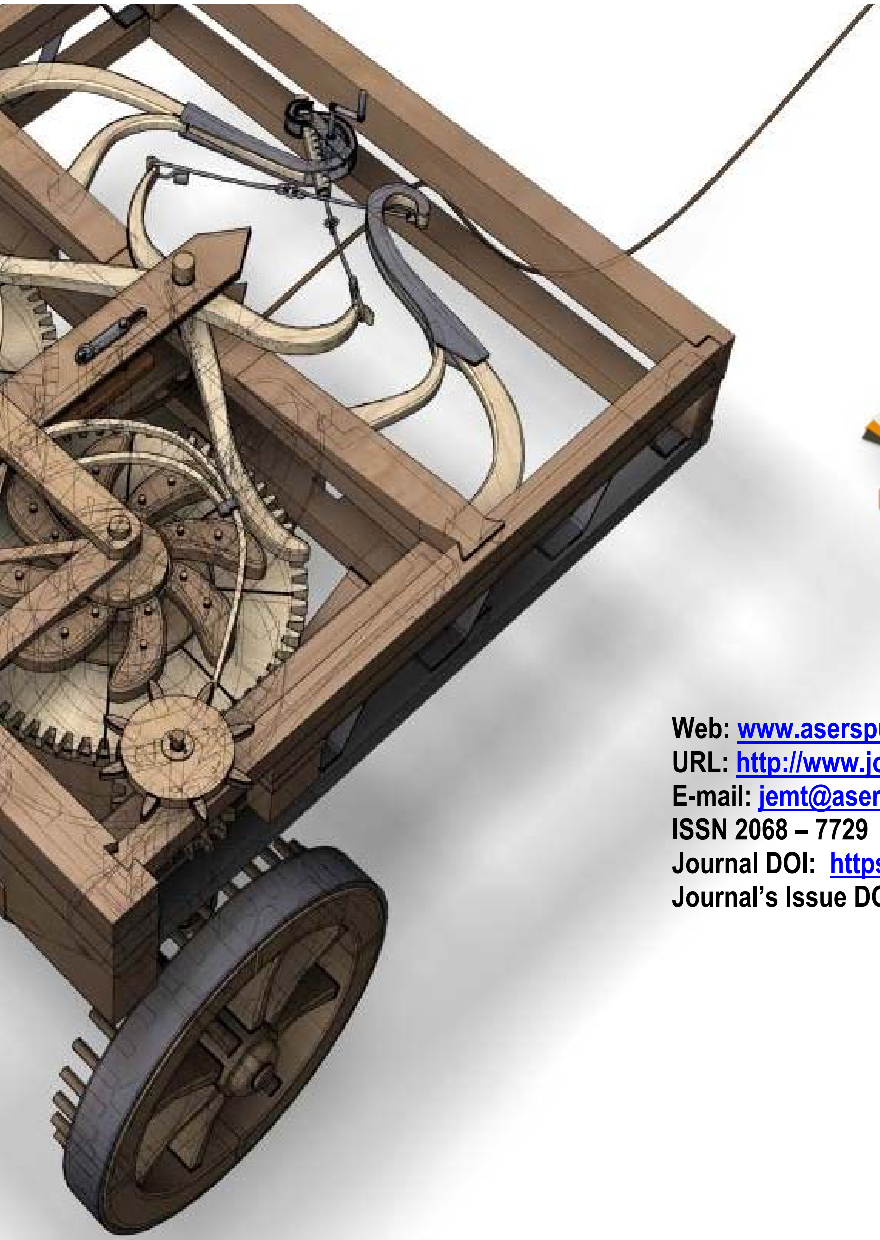

Web: www.aserspublishing.eu
URL: http://www.journals.aserspublishing.eu/jemt
E-mail: jemt@aserspublishing.eu
ISSN 2068 – 7729
Journal DOI: https://doi.org/10.14505/jemt
Journal's Issue DOI: https://doi.org/10.14505/jemt.v10.1(33).00